Production of 3-hydroxy acids from acetate in engineered *Escherichia coli*

by

Bradley Mozell

A thesis

presented to the University of Waterloo

in fulfilment of the

thesis requirement for the degree of

Master of Applied Science

in

Chemical Engineering

Waterloo, Ontario, Canada, 2018

Author’s declaration

I hereby declare that I am the sole author of this thesis. This is a true copy of the thesis, including any required final revisions, as accepted by my examiners. I understand that my thesis may be made electronically available to the public.

Abstract

Acetate serves as an uncommon carbon source for metabolic engineering of value-added chemicals. As a carbon source, acetate has unique advantages since it is not derived from food sources and can be produced as a waste by-product from many biological processes. This allows acetate to be an inexpensive feed source for biomanufacturing whose use would not affect food prices. However, use of acetate as a feed source for bioproduction is limited by its inhibitory effects. As such, fine chemicals, which have high value and low production demand, are preferred target products for bioproduction using acetate feed. 3-hydroxy acids, i.e. 3-hydroxybutyrate (3-HB) and 3-hydroxyvalerate (3-HV), are one such example of fine chemicals. This study demonstrates the production of 3-HB and 3-HV in recombinant *Escherichia coli*, using acetate as a sole carbon source. Various metabolic pathways related to acetate metabolism such as; acetate assimilation, glyoxylate shunt, glycolytic and gluconeogenic pathways related to the phosphoenolpyruvate-pyruvate node, as well as global regulatory systems, were manipulated through targeted gene knockouts, to boost the production of 3-hydroxy acids. These genetic manipulations of the base 3-hydroxy acid-producing strain of *E. coli* resulted in the production of up to 1.75 g/L of 3-HB and 0.571 g/L of 3-HV (individually).

Acknowledgements

First and foremost, I would like to thank my supervisor, Dr. C. P. Chou, for guiding my growth as a graduate student. Your expertise and supervision drove me to constantly learn and improve my critical analysis skills.

I would also like to thank Dr. Simakov, Dr. Ward, and Dr. Moo-Young for serving as my thesis committee. I greatly appreciate you taking time to review my thesis and defense, while providing valuable feedback.

I would like to thank Shane Kilpatrick, and Dragan Miscevic for providing excellent technical training, as well as establishing me as a member of Dr. Chou's research group. Your support and guidance were invaluable during my research and lab work.

Finally. I must thank my friends and family for their endless support throughout this endeavor. Having you cheering me on from Thunder Bay kept me pushing through all the challenges of the MASc program. I would specifically like to thank Emma Koivu for helping me to feel at home while in Waterloo.

Table of contents

List of figures

List of tables

List of abbreviations

3-HB	3-Hydroxybutyrate
3-HB-CoA	3-Hydroxybutyryl-Coenzyme A
3-HV	3-Hydroxyvalerate
3-HV-CoA	3-Hydroxyvaleryl-Coenzyme A
AceA	Isocitrate lyase
AceB	Malate synthase
AceEF	Pyruvate dehydrogenase
AceK	Isocitrate dehydrogenase kinase/phosphatase
AckA	Acetate kinase
AcnAB	Aconitate hydratase
Acs	Acetyl-CoA synthetase
ActP	Acetate permease
ADP	Adenosine diphosphate
AMP	Adenosine monophosphate
ArcA	DNA-binding transcriptional dual regulator protein
ATP	Adenosine Triphosphate
BktB	β-Ketothiolase
CoA	Coenzyme A

CreB	DNA-binding transcriptional regulator
CreC	Sensory histidine kinase
DNA	Deoxyribonucleic acid
Flp	Flippase
Fnr	DNA-binding transcription dual regulator protein
FrdABCD	Fumerate reductase complex
FRT	Flippase recognition target
FumABC	Fumarases A, B, and C
GlcB	Malate synthase
GltA	Citrate synthase
Hbd	3-hydroxybutyryl-CoA dehydrogenase
HPLC	High performance liquid chromatography
Icd	Isocitrate dehydrogenase
IclR	DNA-binding transcriptional repressor protein
IPTG	Isopropyl β-D-1-thiogalactopyanoside
LB	Lysogeny broth
MaeB	Malate dehydrogenase ($NADP^+$-requiring)
Mdh	Malate dehydrogenase
NAD^+	Nicotinamide adenine dinucleotide
NADH	Reduced form NAD^+
$NADP^+$	Nicotinamide adenine dinucleotide phosphate
NADPH	Reduced form $NADP^+$
OAA	Oxaloacetate

OD_{600}	Optical density at 600nm
PckA	Phosphoenolpyruvate carboxykinase
PCR	Polymerase chain reaction
PEP	Phosphoenolpyruvate
PflB	Pyruvate formate lyase
PhaA	Acetoacetyl-CoA thiolase
PhaB	Acetoacetyl-CoA reductase
PhaC	Polyhydroxyalkanoate polymerase/synthase
PHB	Poly(3-hydroxybutyrate)
PHBV	Poly(3-hydroxybutyrate-*co*-3-hydroxyvalerate)
PoxB	Pyruvate oxidase
Ppc	Phosphoenolpyruvate carboxylase
PpsA	Phosphoenolpyruvate synthetase
Pta	Phosphate acetyltransferase
PykF	Pyruvate kinase
RID	Refractive index detector
SatP	Acetate/succinate symporter
Sbm	Methylmalonyl-CoA mutase
SdhCDAB	Succinate:quinone oxidoreductase complex
SfcA	Malate dehydrogenase (NAD^+-requiring)
SucAB	2-ketoglutarate dehydrogenase
SucCD	Succinyl-CoA synthetase
TCA cycle	Tricarboxylic acid cycle

TesB	Acyl-CoA thioesterase
VOC	Volatile organic carbon
YgfG	Methylmalonyl-CoA decarboxylase
YgfH	Propionyl-CoA:succinyl-CoA transferase

List of symbols

Δ	Indicates the succeeding gene was knocked out
Amp^R	Ampicillin resistance
˚C	Degrees Celsius
Cm^R	Chloramphenicol resistance
g	Grams
h	Hours
K_M	Michaelis-Menton constant
Km^R	Kanamycin resistance
L	Liters
mM	Millimolar
pH	Potential of hydrogen
rpm	Revolutions per minute
vvm	Vessel volume per minute

Chapter 1 – Introduction

Organic chemical production has traditionally been performed by the petrochemical industry. Petrochemical operations rely on limited and non-renewable fossil fuels as a feed source. This has sparked interest in bio-manufacturing as a sustainable, alternative production method for organic chemicals (Gavrilescu & Chisti, 2005). Bio-manufacturing utilizes engineered cells, microbes, tissues, or free enzymes to produce commercially significant chemicals from biomass or waste (Yi-Heng Percival Zhang et al., 2017). Recent advancements in genetic engineering, bioinformatics, synthetic biology and metabolic engineering have given rise to novel strategies to exploit microbial fermentation processes for bio-based production of target chemicals (Nielsen & Keasling, 2016). Bio-based production operations rely on these biotechnological strategies to improve existing pathways, or develop novel pathways towards non-native chemical compounds (Schmidt-Dannert, 2017).

In order for bio-manufacturing operations to become economically viable, products that are difficult to produce chemically should be targeted, i.e. fuels, pharmaceuticals, polymers, and fine/platform chemicals. Fine chemicals are a group of complex chemicals (i.e. multiple functional groups, or chiral centres) with high value and limited production rates that are often used as multi-purpose intermediates for other processes (Cybulski et al., 2001). 3-Hydroxy acids are a type of fine chemical defined by a hydroxyl group bonded to the beta-carbon relative to a carboxyl group. Additionally, 3-hydroxy acids contain a chiral centre, making them optical isomers with either (*S*) or (*R*) configurations. These 3-hydroxy acids are used as building blocks for production of antibiotics, vitamins, perfumes and pheromones (Lee & Lee, 2003). Herein, we demonstrated production of 3-hydroxybutyrate (3-HB) and 3-hydroxyvalerate (3-HV) in engineered *Escherichia coli* using acetate as the sole carbon source. 3-HB and 3-HV also have applications as monomers

for biodegradable plastics (Srirangan et al., 2016) i.e. poly(3-hydroxybutyrate) (PHB) and poly(3-hydroxybutyrate-*co*-3-hydroxyvalerate) (PHBV). However, PHB has limited applications since, as a homopolymer, it has high crystallinity making it brittle and hard. PHB also has a high melting temperature limiting its workability (Wang et al., 2013). Incorporation of 3-HV into the copolymer PHBV, allows more desirable properties i.e. better impact resistance, toughness, flexibility, and decreased melting point (Wang et al., 2013).

Acetate has gained attention as an alternative, non-food related substrate for biomanufacturing (Huang et al., 2018). As a common fermentative by-product, acetate has potential as an economical carbon source since it is often seen as a waste chemical of microbe-based biomanufacturing. Acetate can also be sustainably produced by syngas fermentations or by lignocellulosic refineries (Chong et al., 2013; Munasinghe and Khanal (2010); Y-H Percival Zhang, 2008). *E. coli* can grow using acetate as a substrate by first transporting acetate into the cytosol by the acetate permease, ActP (encoded by *actP*) or the acetate/succinate symporter, SatP (encoded by *satP*) (Gimenez et al., 2003; Sá-Pessoa et al., 2013). Intracellular acetate can be assimilated into central metabolism as acetyl-CoA by either the Acs pathway or the AckA-Pta pathway as shown in **Figure 1**. Acetyl-CoA acts as a precursor for many natural metabolic pathways (Castaño-Cerezo et al., 2009), i.e. incorporated in the tricarboxylic acid (TCA) cycle via fusion with either glyoxylate or oxaloacetate(OAA) to form malate or citrate respectively. Acetyl-CoA can also be used, a vital precursor for 3-HB and 3-HV biosynthesis, as shown in **Figure 2**. However, biosynthesis of 3-HV also requires non-native propionyl-CoA in addition to acetyl-CoA (**Figure 2**). Typically, 3-HV biosynthesis requires supplementation of a structurally similar carbon source to generate propionyl-CoA, i.e. valerate, or propionate (Doi et al., 1988; Tseng et al., 2010). However, by activating the dormant Sleeping beauty mutase (Sbm) operon present in *E. coli*,

propionyl-CoA can be produced independent of carbon source (Akawi et al., 2015). The Sbm pathway diverts succinyl-CoA from the TCA cycle to L-methylmalonyl-CoA then subsequently to propionyl-CoA (**Figure 1**).

Acetate has previously been used as a sole carbon source for metabolite production in *E. coli*, i.e. MNEI, succinate, itaconic acid, and propionate (Leone et al., 2015; Li et al., 2016; Noh et al., 2018; Kilpatrick 2017). A comparison of the results from these studies can be found below in **Table 1.** Additionally, results from previous studies demonstrating production of 3-HB and 3-HV can be found in **Table 2**. However, it should be noted that until this study, acetate has not been used as a feedstock for the production either 3-HB or 3-HV.

Utilizing acetate as a carbon source drastically affects the central metabolism pathway of *E. coli* by inducing the activation of the glyoxylate shunt and gluconeogenic pathways, influencing multiple regulator systems, and down-regulating glycolytic pathways (Oh et al., 2002). To determine the significance and effects of different metabolic pathways on 3-hydroxy acid production specific gene knockouts related to the acetate assimilation pathways, glyoxylate shunt, phosphoenolpyruvate (PEP)-pyruvate node, and global regulator systems, were investigated. This study demonstrated the production of 3-HB and 3-HV with titers up to 1.75 g/L and 0.571 g/L, respectively, using acetate as a sole carbon source in genetically engineered strains of *E. coli*.

Table 1: Comparison of this study with previous studies using acetate as a sole feed source for metabolite production in *E. coli*

Product	**Feedstock**	**Study**
1.75 g/L 3-HB and 0.571 g/L 3-HV	20 g/L acetate	This Study
177 mg/L of MNEI	4.6 g/L acetate	(Leone et al., 2015)
7.3 g/L succinate	14.4 g/L acetate	(Li et al., 2016)
3.57 g/L itaconic acid	10 g/L acetate	(Noh et al., 2018)
3.8 g/L propionate	20 g/L acetate	(Kilpatrick 2017)

Table 2: Comparison of this study with previous studies for 3-hydroxy acid productions from unrelated carbon sources

Products	**Host organism**	**Feed Stock**	**Study**
1.75 g/L 3-HB and 0.571 g/L 3-HV	*E. coli*	20 g/L acetate	This Study
4.84 g/L 3-HB	*Arxula adeninvorans*	50 g/L glucose	(Biernacki 2017)
2.1 g/L 3-HB	*E. coli*	20 g/L glucose	(Gao 2002)
2.99 g/L 3-HB and 2.29 g/L 3-HV	*E. coli*	30 g/L glycerol	(Miscevic 2018)

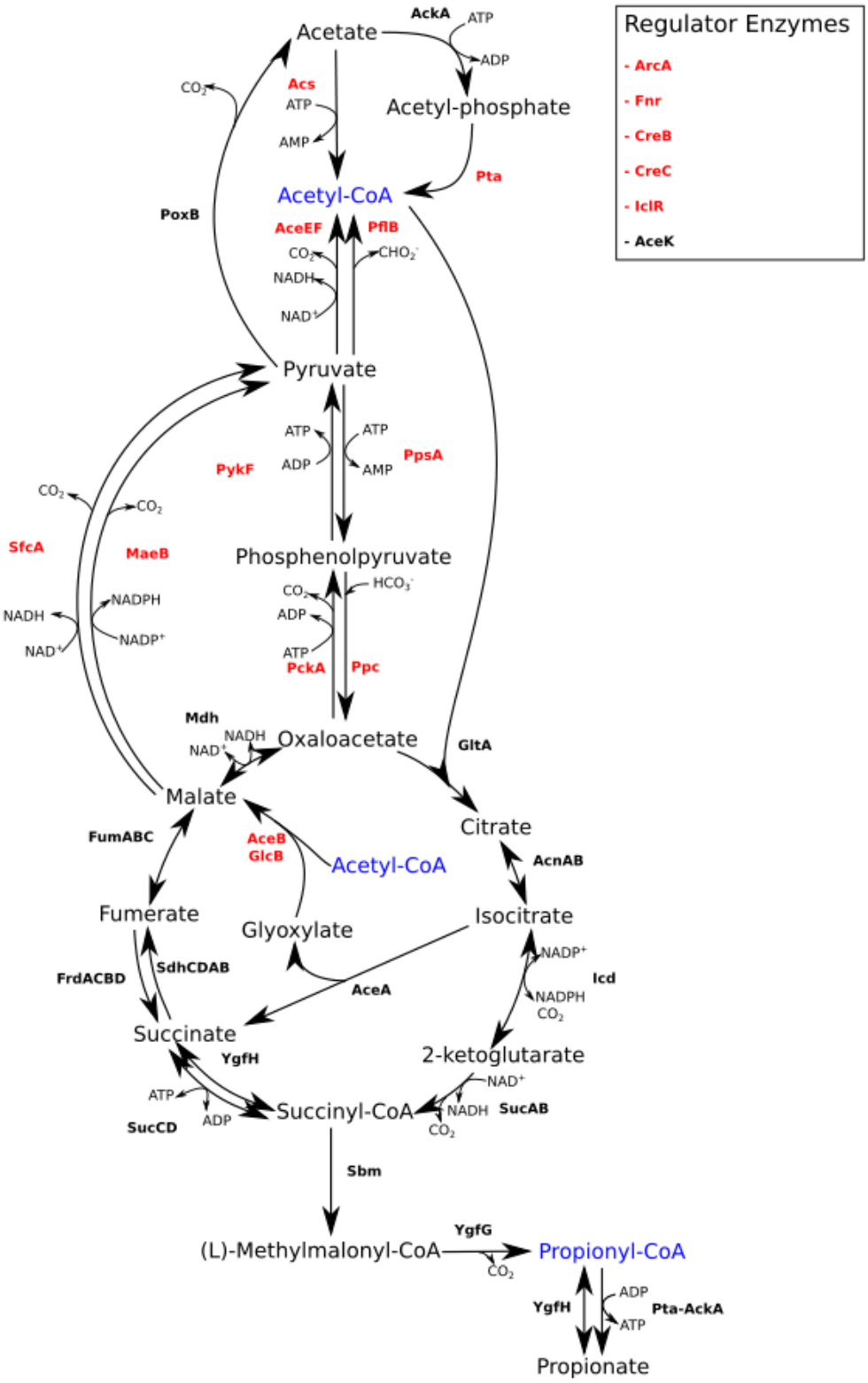

Figure 1: Schematic representation of natural and engineered pathways for acetate metabolism in CPC-Sbm. It should be noted that enzymes in red were investigated in this study through the

knockout of their coding gene. Acetyl-CoA and propionyl-CoA are shown in blue as they are necessary precursors for the biosynthesis of 3-HB and 3-HV. Enzyme abbreviations: ArcA, DNA-binding transcriptional dual regulator; Fnr, DNA-binding transcriptional dual regulator; CreB, DNA-binding transcriptional regulator; CreC, sensory histidine kinase; IclR, DNA-binding transcriptional repressor; AceK, isocitrate dehydrogenase kinase/phosphatase; AckA, acetate kinase; Pta, phosphate acetyltransferase; Acs, acetyl-CoA sythetase; PoxB, pyruvate oxidase; AceEF, pyruvate dehydrogenase; PflB, pyruvate formate lyase; PykF, pyruvate kinase; PpsA, phosphoenolpyruvate synthetase; SfcA, malate dehydrogenase (NAD+-requiring); MaeB, malate dehydrogenase (NADP+-requiring); PckA, phosphoenolpyruvate carboxykinase; Ppc, phosphoenolpyruvate carboxylase; Mdh, malate dehydrogenase; GltA, citrate synthase; AcnAB, aconitate hydratase; Icd, isocitrate dehydrogenase; SucAB, 2-ketoglutarate dehydrogenase; SucCD, succinyl-CoA synthetase; SdhCDAB, succinate:quinone oxidoreductase; FrdABCD, fumerate reductase; FumABC, fumerase; AceA, isocitrate lyase; AceB, malate synthase; GlcB, malate synthase; Sbm, methylmalonyl-CoA mutase; YgfG, methylmalonyl-CoA decarboxylase; YgfH, propionyl-CoA:succinyl-CoA transferase.

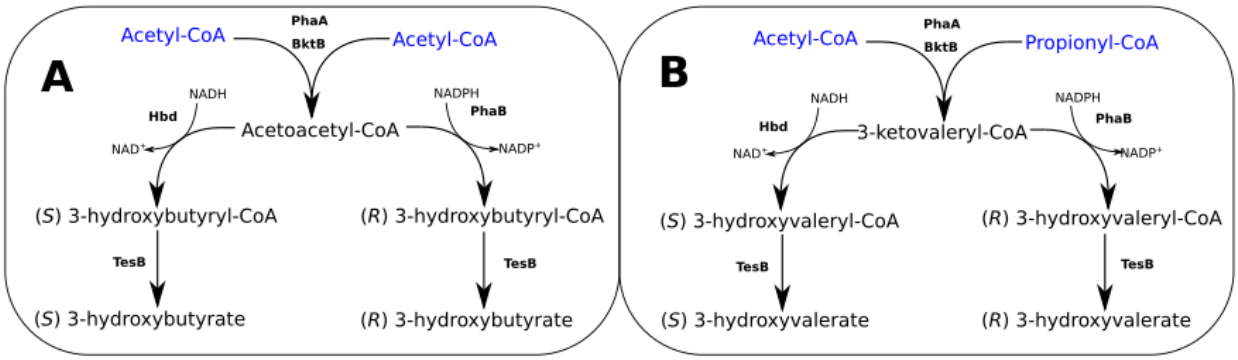

Figure 2: Heterologous 3-HB (A) and 3-HV (B) pathways from acetyl-CoA and propionyl-CoA precursors. Enzyme abbreviations: PhaA, acetoacetyl-CoA thiolase (from *C. necator*); BktB, ß-ketothiolase (from *C. necator*); Hbd, 3-hydroxybutyryl-CoA dehydrogenase (from *C. acetobutylicum*); PhaB, acetoacetyl-CoA reductase (from *C. necator*); TesB, acyl-CoA thioesterase (from *E. coli*).

Chapter 2 - Materials and methods

2.1 - Bacterial strains and plasmids

A list of all *E. coli* strains, plasmids and DNA primers used in this study can be found in **Table 1**. Genomic DNA from various bacterial strains was isolated using the Blood & Tissue DNA Isolation Kit (Qiagen, Hilden, Germany). Standard recombinant DNA technologies were applied for molecular cloning (Miller, 1993). All plasmids were constructed by Gibson enzymatic assembly (Gibson et al., 2009). Phusion HF and *Taq* DNA polymerases were obtained from New England Biolabs (Ipswich, MA, USA). All synthesized oligonucleotides were obtained from Integrated DNA Technologies (Coralville, IA, USA). DNA sequencing was conducted by the Centre for Applied Genomics at the Hospital for Sick Children (Toronto, Canada). *E. coli* BW 25113 was the parental strain for derivation of all mutant strains in this study and *E. coli* DH5α was used as a host for molecular cloning.

Activation of the genomic Sbm operon to generate propionogenic (propionate-producing) *E. coli*, CPC-Sbm was described previously (Srirangan et al., 2014). Knockouts of the genes, were introduced into CPC-Sbm by P1 phage transduction (Miller, 1993) using the appropriate Keio Collection strains (The Coli Genetic Stock Center, Yale University, New Haven, CT, USA) as donors (Baba et al., 2006). To eliminate the co-transduced FRT-Kn^R-FRT cassette, the transductants were transformed with pCP20 (Cherepanov & Wackernagel, 1995), a temperature sensitive plasmid expressing a flippase (Flp) recombinase. Upon Flp-mediated excision of the Kn^R cassette, a single Flp recognition site (FRT "scar site") was generated. Plasmid pCP20 was then removed by growing cells at 42°C. The genotypes of derived knockout strains were confirmed by colony PCR using the appropriate verification primer sets.

The *phaAB* operon was amplified by polymerase chain reaction (PCR) using the primer set g-phaAB and the genomic DNA (gDNA) of wild-type *Cupriavidus necator* ATCC 43291 as the template. The amplified operon was Gibson–assembled (Note that "assembled" is used for subsequent appearance) with the PCR-linearized pTrc99a using the primer set g-pTrc-phaAB to generate pTrc-PhaAB. All genes inserted into pTrc99a vector were under the control of the P_{trc} promoter. Plasmid pK-BktB-Hbd-TesB was previously constructed in our lab by PCR-amplifying *bktB* from *C. necator* ATCC 43291, *hbd* from *Clostridium acetobutylicum* ATCC 824, and *tesB* from *E. coli* BW 25141 using the corresponding primer sets (i.e. g-bktB, g-hbd, and g-tesB), followed by assembling all three PCR-amplified fragments with the PCR-linearized pK184 using the primer set g-pK-bktB-hbd-tesB. All genes inserted into pK184 vector were under the control of the P_{lac} promoter. The two plasmids, pTrc-PhaAB and pK-BktB-Hbd-TesB, were transformed into the propionogenic host strain, CPC-Sbm, to generate the 3-hydroxy acid producing strain, P3HA31.

Table 3: List of *E. coli* strains, plasmids and DNA primers used in this study

Name	Description, relevant genotype or primer sequence (5'→3')	Reference
E. coli host strains		
DH5α	F−, *endA1, glnV44, thi-1, recA1, relA1, gyrA96, deoR, nupG φ80d lacZ*Δ *M15,* Δ*(lacZYA – argF) U169, hsdR17(rK-mK +), λ-*	Lab stock
MC4100	F-, [*araD139*]B/r, Del(*argF-lac*)169, λ–-, e14-, *flhD5301*, Δ(*fruK-yeiR*)*725*(*fruA25*), *relA1*, *rpsL150*(strR), *rbsR22*, Del(*fimB-fimE*)*632*(::IS1), *deoC1*	(Casadaban, 1976)
BW25141	F⁻, Δ(*araD-araB*)567, Δ*lacZ4787*(::*rrnB-3*), Δ(*phoB-phoR*)*580*, *λ-*, *galU95*, Δ*uidA3*::pir+, *recA1*, *endA9*(del-ins)::FRT, *rph-1*, Δ(*rhaD-rhaB*)*568*, *hsdR514*	(Datsenko & Wanner, 2000)
BW25113	F⁻, Δ(*araD-araB*)*567*, Δ*lacZ4787*(::*rrnB-3*), *λ*⁻, *rph-1*, Δ(*rhaD-rhaB*)*568*, *hsdR514*	(Datsenko & Wanner, 2000)
BWΔldhA	BW25113Δ*ldhA* null mutant	(Akawi et al., 2015; Srirangan et al., 2013)
CPC-Sbm	BWΔ*ldhA*, P_{trc}::*sbm* (i.e. with the FRT -P_{trc} cassette replacing the 204-bp upstream of the Sbm operon)	(Akawi et al., 2015)
P3HA31	CPC-Sbm/pTrc-PhaAB and pK-BktB-Hbd-TesB	(Miscevic, 2018)
P3HA31Δ*pta*	*pta* null mutant of P3HA31	(Miscevic, 2018)
P3HA31Δ*acs*	*acs* null mutant of P3HA31	This study
P3HA31Δ*aceB*	*aceB* null mutant of P3HA31	This study
P3HA31Δ*glcB*	*glcB* null mutant of P3HA31	This study
P3HA31Δ*aceB*Δ*glcB*	*aceB* and *glcB* null mutant of P3HA31	This study
P3HA31Δ*iclR*	*iclR* null mutant of P3HA31	This study

P3HA31Δ*sfcA*	*sfcA* null mutant of P3HA31	This study
P3HA31Δ*maeB*	*maeB* null mutant of P3HA31	This study
P3HA31Δ*pckA*	*pckA* null mutant of P3HA31	This study
P3HA31Δ*ppsA*	*ppsA* null mutant of P3HA31	This study
P3HA31Δ*ppc*	*ppc* null mutant of P3HA31	This study
P3HA31Δ*pykF*	*pykF* null mutant of P3HA31	This study
P3HA31Δ*aceF*	*aceF* null mutant of P3HA31	This study
P3HA31Δ*pflB*	*pflB* null mutant of P3HA31	This study
P3HA31Δ*arcA*	*arcA* null mutant of P3HA31	This study
P3HA31Δ*fnr*	*fnr* null mutant of P3HA31	This study
P3HA31Δ*creB*	*creB* null mutant of P3HA31	This study
P3HA31Δ*creC*	*creC* null mutant of P3HA31	This study
CPC-PHBV	CPC-Sbm/pTrc-PhaCAB and pK-BktB	(Srirangan et al., 2016)
Plasmids		
pCP20	FLP^+, λ $cI857^+$, λ p_R Rep(pSC101 ori)^{ts}, Ap^R,Cm^R	(Cherepanov & Wackernagel, 1995)
pKD46	Rep$A101^{ts}$ ori, Ap^R, *araC*-P_{araB}::*gam-bet-exo*	(Datsenko & Wanner, 2000)
pKD3	R6K-γ ori, Ap^R, FRT-Cm^R-FRT	(Datsenko & Wanner, 2000)
pTrc99a	ColE1 ori Apr P*trc*	(Amann et al., 1988)

pK184	p15A ori, Km^R, P_{lac}::*lacZ'*	(Jobling & Holmes, 1990)
pTrc-PhaAB	Derived from pTrc99a, P_{trc}:: *phaAB*	(Miscevic, 2018)
pK-BktB-Hbd-TesB	Derived from pK184, P_{lac}:: *bktB:hbd:tesB*	(Miscevic, 2018)
Primers		
v-ldhA	GATAACGGAGATCGGGAATGATTAA; GGTTTAAAAGCGTCGATGTCCAGTA	(Srirangan et al., 2013)
v-pta	GGCATGAGCGTTGACGCAATCA; CAGCTGTACGCGGTGATACTCAGG	(Akawi et al., 2015)
v-acs	ACTTTTGCGTGATCTGTCGC; CTCCAGAGGTAATGTAGGGA	This study
v-aceB	TTTCCGAAACGTACCTCAGC; CATTTTCGCTGCGCCCAGTT	This study
v-glcB	GCAGACGCAGAGTATCGTTA; ACAACGGACGTACCGCGTTC	This study
v-iclR	GGTGGAATGAGATCTTGCGA; CCGACACGCTCAACCCAGAT	This study
v-sfcA	TCAGTGAGCGCAGTGTTTTA; AACCCAACCGGCAGAAAACG	This study
v-maeB	TGGAGAGATATTCGCTGTGG; GACAGGCATGGTATTGCTGG	This study
v-pckA	CCGTTTCGTGACAGGAATCA; AACGGGATGCTGGAGCTTGG	This study
v-ppsA	CGCGAACTACCTCAGGTA AA; CGAAGAGAGCAGATTTGCGC	This study
v-ppc	CGCCGAATGTAACGACAATTCC; TGCTGAAGCGATTTCGCAGC	This study
v-pykF	GGACTGTAGAACTCAACGAC; GCGTTCGATGCTTCTTTGAG	This study
v-aceF	TGCGTCACCACTTCGAAGTT; GGATTTCTGGGTGCAGCAAG	This study
v-pflB	ATTTTGGACCGCAGTCGGTT; CGGTTCCACAGGATTCAAAG	This study
v-arcA	TTGGGAACCAGTGTGCTGGT; ACTGTCGGGTCCTGAGGGAA	This study
v-fnr	GTGCCAGCTTGTTCACACTT; TGGGAACGCCAGCATTGAGA	This study
v-creB	CGATTGAACTGTCGGATCGT; AACGTTGCGGTGTCGATCAA	This study

v-creC	CGCTGACTCGGTATGAGTTT; TCAGCACGTTCGACAATCAC	This study
c-ptrc	CCGATTCATTAATGCAGCTGG; GGTCTGTTTCCTGTGTGAAATTGTTA	This study
c-pK184	ATGACCATGATTACGAATTCG; AGCTGTTTCCTGTGTGAAATTGTTATCCG	This study
g-phaA	**CCGGCTCGTATAATGTGTGG**ATGACTGACGTTGTCATCGTATCC; **TACCGAGCTCGAATTCC**TTATTTGCGCTCGACTG	(Miscevic, 2018)
g-phaB	**TTCACACAGGAAACAGAC**ATGACTAGCGCATTGCGT; **GGTACCGAGCTCGAATTCCATG**TCAGCCCATATGCAGGCC	(Miscevic, 2018)
g-phaAB	**CCGGCTCGTATAATGTGTGG**ATGACTGACGTTGTCATCGTATCC; **ATTGTTATCCGCTCACAATT**TCAGCCCATATGCAGGCCGA	(Miscevic, 2018)
g-bktB	**CACAGGAAACAGCTATGACC**ATGACGCGTAAGTGGTAGT; **TAAACAGACCTCCCTTAAATTTAAT**TCAGATACGCTCGAAGATGG	(Miscevic, 2018)
g-hbd	**TTAAATTTAAGGGAGGTCTGTTTA**ATGAAAAAGGTATGTGTTATAGG; **TAACAAAGCTGCCGCAG**TTATTTTGAATAATCGTAGAAACCTTT	(Miscevic, 2018)
g-tesB	**GCTTTGTTACTGGAGAGTTAT**ATGAGTCAGGCGCTAAAAA; **GAGCTCGAATTCGTAATCA**TTAATTGTGATTACGCATCAC	(Miscevic, 2018)
g-pTrc-phaAB	GCGGCCTGCATATGGGCTGA**TGGAATTCGAGCTCGGTACC**; ACGATGACAACGTCAGTCAT**GTCTGTTTCCTGTGTGAAATTGTTATCCG**	(Miscevic, 2018)
g-pK-bktB-hbd-tesB	**GGTGATGCGTAATCACAATTAA**TGATTACGAATTCGAGCTCGG; **TACCACTTCACGCGTCAT**GGTCATAGCTGTTTCCTGTGTGAA	(Miscevic, 2018)

Notation for primers: v- verification primer, **c**- cloning primer, and **g**-Gibson DNA assembly primer. Homology arms are in bold

2.2 - Media and cultivations

All medium components were obtained from Sigma-Aldrich Co. (St Louis, MO, USA) except yeast extract, and tryptone, which were obtained from BD Diagnostic Systems (Franklin Lakes, NJ, USA). The media were supplemented with antibiotics as required: 25 µg/mL kanamycin and 50 µg/mL ampicillin. *E. coli* strains, stored as glycerol stocks at -80 °C, were streaked on lysogeny broth (LB) agar plates with appropriate antibiotics and incubated at 37°C for 14-16 h. Single colonies were picked from LB plates to inoculate 30-mL LB medium (10 g/L tryptone, 5 g/L yeast extract, and 5 g/L NaCl) with appropriate antibiotics in 125-mL conical flasks. The cultures were shaken at 37°C and 280 rpm in a rotary shaker (New Brunswick Scientific, NJ, USA) and used as seed cultures to inoculate 200 mL LB media at 1% (v/v) with appropriate antibiotics in 1-L conical flasks. This second seed culture was shaken at 37°C and 280 rpm until an optical density of 0.80 OD_{600} was reached. Cells were then harvested by centrifugation at 9,800 ×g and 20°C for 10 min and resuspended in 30-mL modified M9 production media. The suspended culture was transferred into three identical 125-mL screw cap plastic production flasks (10mL of culture per flask) and incubated at either 30°C or 37°C at 280 rpm in a rotary shaker. Unless otherwise specified, the modified M9 production medium contained 27.78 g/L sodium acetate (to yield 20 g/L acetate), 5 g/L yeast extract, 10 mM $NaHCO_3$, 1 mM $MgCl_2$, 0.2 µM cyanocobalamin (vitamin B12), 5^{th} dilution of M9 salts mix (33.9 g/L Na_2HPO_4, 15 g/L KH_2PO_4, 5 g/L NH_4Cl, 2.5 g/L NaCl), $1{,}000^{th}$ dilution of Trace Metal Mix A5 (2.86 g/L H_3BO_3, 1.81 g/L $MnCl_2{\bullet}4H_2O$, 0.222 g/L $ZnSO_4{\bullet}7H_2O$, 0.39 g/L $Na_2MoO_4{\bullet}2H_2O$, 79 µg/L $CuSO_4{\bullet}5H_2O$, 49.4 µg/L $Co(NO_3)_2{\bullet}6H_2O$), and supplemented with 0.1 mM isopropyl-β-D-1-thiogalactopyranoside (IPTG). It should be noted this media was controlled to a pH of 7 prior to cultivation, by addition of 5 M H_2SO_4 while measuring pH with a benchtop pH meter. All cultivation experiments were performed in triplicate.

2.3 - Offline analysis and metabolite quantification

Culture samples were appropriately diluted with 0.15 M saline solution for measuring the optical cell density (OD_{600}) using a spectrophotometer (DU520, Beckman Coulter, Fullerton, CA). Cell-free medium was collected by centrifugation of the culture sample at 10,000 ×g and filter sterilized for titer analysis of acetate, and various metabolites using a high-performance liquid chromatography (HPLC; LC-10AT, Shimadzu, Kyoto, Japan) with a refractive index detector (RID; RID-10A, Shimadzu, Kyoto, Japan) and a chromatographic column (Aminex HPX-87H, Bio-Rad Laboratories, CA, USA). The HPLC column temperature was maintained at 35 °C and the mobile phase was 5 mM H_2SO_4 (pH 2.0) running at 0.6 mL/min. The RID signal was acquired and processed by a data processing unit (Clarity Lite, DataApex, Prague, Czech Republic).

2.4 – Proposed methods for industrial production of 3-hydroxy acid products

A proposed process flow diagram for industrial biomanufacturing of 3-hydroxyacid products can be found below in **Figure 3.** Initially a seed culture is inoculated from a microbe stock stored at -80˚C. Next the seed culture is used to initiate a production fermenter where the cultivation would be carried out to produce the desired products. The fermenter effluent must then be treated by separation processes to remove cells, remove contaminants, isolate and finally purify the 3-hydroxy acid products. Initially, microbe cells would be removed from the liquid effluent by centrifugation and filtration (Shuler & Kargi 2002). Next the cell-free media can be subjected to activated carbon adsorption to remove contaminants (i.e., volatile organic carbons (VOCs) and heavy metals) from the media. 3-hydroxy acids can be separated from the other media components by a combination of extraction, distillation and/or precipitation processes (Li et al., 2015). Extraction utilizes a solvent to dissolve the 3-hydroxy acids but is immiscible with water allowing distinct phases to separate the 3-hydroxy acids from the aqueous mixture. Additionally,

reactive extraction can be performed by performing an esterification reaction on 3-hydroxy acids to increase the extraction efficiency (Li et al., 2015). Distillation can be used to separate media components based on the volatility of the components. Distillation can be used to vaporize water and volatile compounds to separate them from the less volatile 3-hydroxy acids (Li et al., 2015). 3-hydroxy acids may also be precipitated from liquid media using the addition of calcium to create insoluble calcium salts of 3-hydroxy acids. The solid precipitates can then be filtered from the liquid media (Li et al., 2015). These methods can effectively separate 3-hydroxy acids from most other media components, however purification of 3-HB and 3-HV as well as enantiomeric separation requires further processing. Chiral chromatography using an ion-exchange column (i.e., Chiralpak QN-AX, and Chiralpak ZWIX(+)) can effectively isolate 3-HB and 3-HV while also separating (*R*) and (*S*) enantiomers of both compounds (Ianni et al., 2014). Separation of 3-HB and 3-HV enantiomers may also be accomplished by coupled preferential crystallization (Chaaban et al., 2014). This process operates by passing a mixed feed stream through a pair of crystallization vessels. Each vessel preferentially crystalizes either (*R*) or (*S)* enantiomers yielding solid purified products (Chaaban et al., 2014). Finally, the purified 3-HB and 3-HV undergo drying to remove any residual water then packaging and distribution to the consumer.

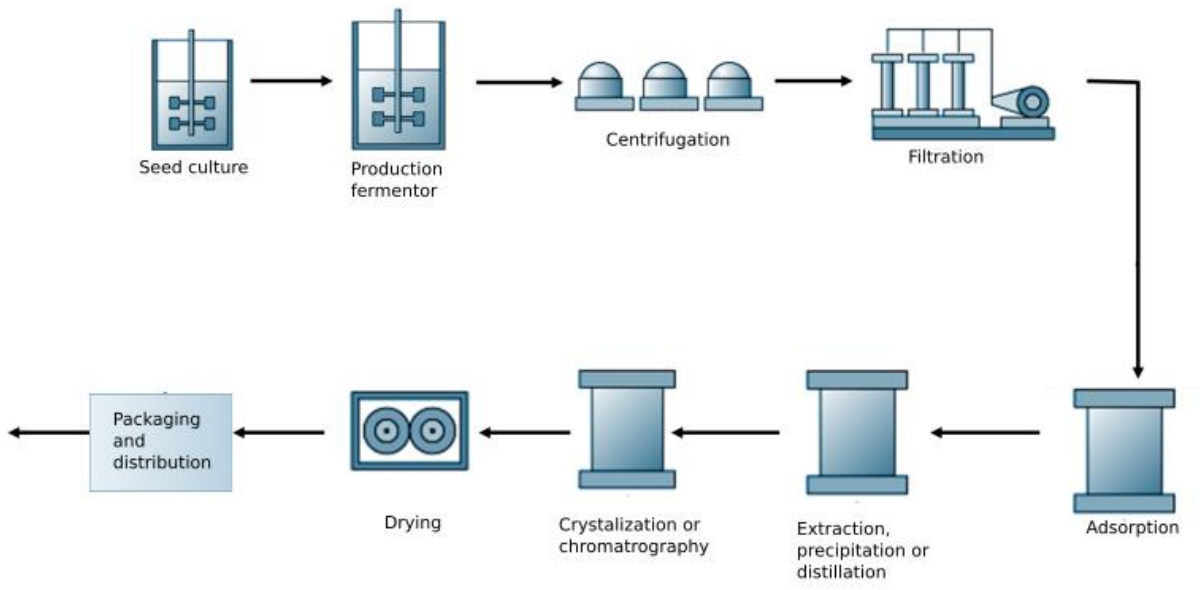

Figure 3: A process flow diagram describing the proposed process for bio-production of 3-HB and 3-HV.

Chapter 3 – Results

3.1 - Heterologous expression of 3-hydroxy acid pathway

3-HB and 3-HV are non-native products from *E. coli* metabolism, therefore multiple genetic engineering strategies are required to effectively produce 3-HB and 3-HV. The physiologically dormant Sleeping beauty mutase (Sbm) operon was previously activated in the *E. coli* host strain, to yield the propionogenic strain, CPC-Sbm. The Sbm pathway acts on succinyl-CoA to divert carbon from the TCA cycle and produce propionyl-CoA, an essential precursor for odd-chain metabolite production, i.e. 3-HV (Akawi et al., 2015; Miscevic, 2018; Srirangan et al., 2014). The optimum 3-hydroxy acid producing strain, P3HA31 (Miscevic, 2018) was generated by heterologous expression of the 3-hydroxy acid-pathway (**Figure 2)** in a double plasmid system. The first step of the pathway consists of either the homo-fusion of 2 acetyl-CoA moieties or the hetero-fusion of acetyl-CoA and propionyl-CoA to form acetoacetyl-CoA or 3-ketovaleryl-CoA

respectively. The fusion reaction is carried out by either the β-ketothiolase, BktB, (encoded by *bktB*) or by the acetyl-CoA acetyltransferase, PhaA, (encoded by *phaA*). In the second step, acetoacetyl-CoA and 3-ketovaleryl-CoA are reduced to both (*R*) and (*S*) enantiomers of 3-hydroxybutyryl-CoA (3-HB-CoA) and 3-hydroxyvaleryl-CoA (3-HV-CoA) respectively. The NADH-dependent 3-HB-CoA dehydrogenase, Hbd (encoded by *hbd*) catalyzes the reduction to specifically form (*S*) enantiomers, whereas the NADPH-dependent acetoacetyl-CoA reductase, PhaB (encoded by *phaB*) catalyzes the reduction to specifically form (*R*) enantiomers. In the final step of the 3-hydroxy acid pathways, 3-HB-CoA and 3-HV-CoA undergo hydrolysis via an enantiomerically independent thioesterase, TesB (encoded by *tesB*) to form both enantiomers of 3-HB and 3-HV, respectively.

3.2 - Manipulation of cultivation conditions

Cultivation conditions, specifically temperature and initial carbon source concentrations, were explored to determine their effects on 3-hydroxy acid productions. P3HA31 was cultivated at 30˚C and 37˚C and the results are shown in **Table 4**. The 30˚C culture produced both 3-hydroxy acids at significantly higher titers and yields than the culture at 37˚C. It was necessary to determine an appropriate concentration of acetate in the initial cultivation medium, since accumulation of acetate can inhibit growth and metabolite production of cell cultures (De Mey et al., 2007). Cultivations were performed using 10, 20, and 30 g/L of acetate as the sole carbon source in the media, as shown in **Table 5**. At 10 and 20 g/L of acetate in the media, the growth and product yields for P3HA31 were similar to each other. Acetate inhibition was not significant at these concentrations since over 90% of the initial acetate was consumed in these cultivations. However, when P3HA31 was cultivated at 30 g/L acetate, the growth was significantly inhibited, 3-hydroxy acid titers were lower than at 20 g/L acetate, and approximately 20% of the initial acetate was

consumed (**Figure 4**). These results are corroborated by previous research using acetate for cultivations of CPC-Sbm (Kilpatrick 2017). The researchers also observed inhibition of cell growth and metabolite productions at 30 g/L of acetate, whereas this inhibition was not observed at 20 g/L of acetate. Therefore, 20 g/L of acetate in media was favoured to enhance production of both 3-hydroxy acids without significantly inhibiting the cell growth or product yield.

Table 4: Growth data and metabolite profile of P3HA31 cultivations at different temperatures.

Temperature	**Cell density (OD_{600})[a]**	**Acetate consumed (g/L)[b]**	**Metabolites produced (g/L)[c]**		
			3-HB	**3-HV**	**Propionate**
30˚C	8.99 ± 0.39	16.6 ± 0.6	0.563 ± 0.028 (4.0%)	0.527 ± 0.059 (4.9%)	2.22 ± 0.48 (21.8%)
37˚C	7.01 ± 0.39	15.1 ± 0.6	0.510 ± 0.047 (3.9%)	0.389 ± 0.022 (3.5%)	1.34 ± 0.07 (14.4%)

[a] Measured cell density after 48h cultivation using spectrophotometer (OD_{600}) initial cell densities were kept at ~5.0

[b] Consumed acetate after 48h cultivation (20 g/L initial concentration)

[c] Metabolites produced after 48h cultivation, yield is presented in parentheses as a percentage of theoretical maximum yield based on acetate consumed (%)

Table 5: Growth data and metabolite profile of P3HA31 grown in different acetate concentrations.

Initial acetate concentration in media (g/L)	**Cell density (OD_{600})[a]**	**Acetate consumed (g/L)[b]**	**Metabolites produced (g/L)[c]**		
			3-HB	**3-HV**	**Propionate**
10	9.3	10	0.285 (3.3%)	0.249 (3.8%)	1.704 (27.6%)
20	9.39	18.3	0.562 (3.6%)	0.571 (4.8%)	2.92 (25.9%)
30	4.28	6.4	0.471 (8.5%)	N.D.[d]	0.319 (8.0%)

[a] Measured cell density after 48h cultivation using spectrophotometer (OD_{600}) initial cell densities were kept at ~5.0

[b] Consumed acetate after 48h cultivation

[c] Metabolites produced after 48h cultivation, yield is presented in parentheses as a percentage of theoretical maximum yield based on acetate consumed (%)

[d] No 3-HV was detected as the 3-HV peak could not be accurately separated from the acetate peak

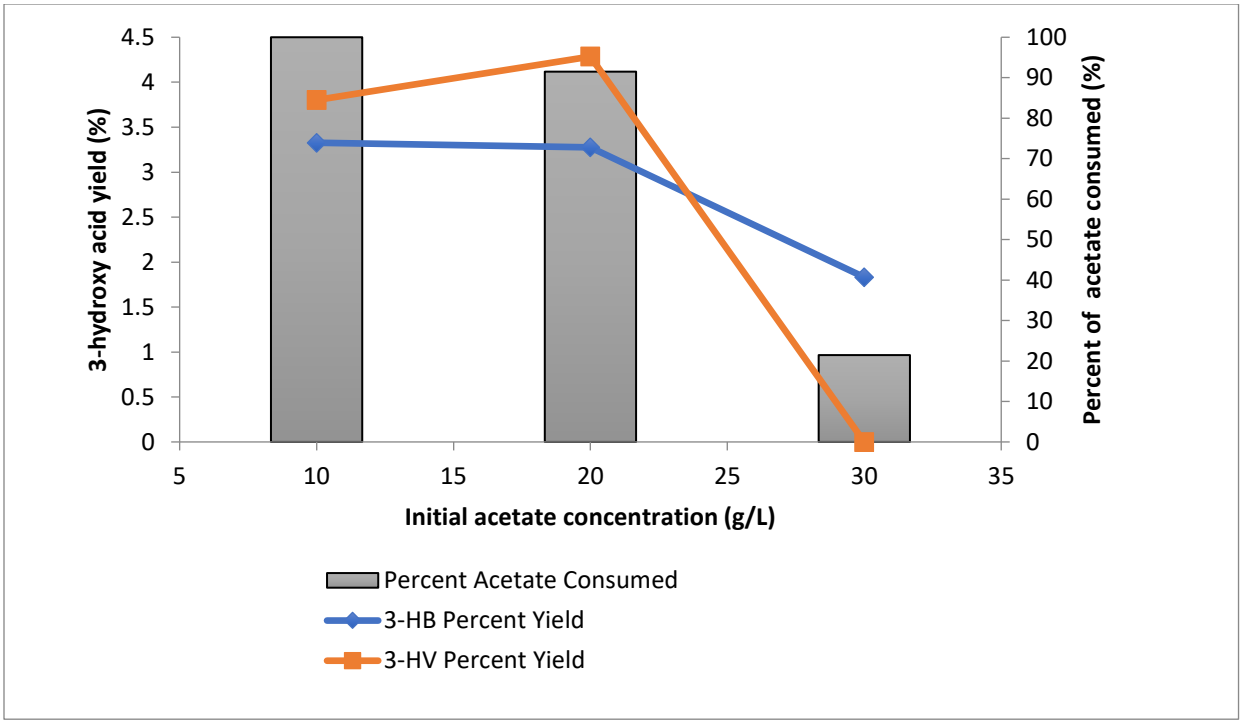

Figure 4: A graph comparing the percent yield of 3-hydroxy acids produced and percent of acetate consumed for P3HA31 cultivated with different initial acetate concentrations in the cultivation media.

3.3 - Genetic manipulation of acetate assimilation pathways

Acetate assimilation occurs via two distinct pathways: (i) acetate is converted to acetyl-phosphate by the acetate kinase, AckA, (encoded by *ackA*) then to acetyl-CoA by the phosphate acetyltransferase, Pta, (encoded by *pta*) in the AckA-Pta pathway, or (ii) acetate is directly converted to acetyl-CoA by the acetyl-CoA sythetase, Acs, (encoded by *acs*). The metabolite profiles and growth data for these gene knockouts is given in **Table 6** and the relative 3-hydroxy acid productions are shown in **Figure 5**. In P3HA31Δ*pta*, the AckA-Pta pathway was inactivated and the mutant had negligible 3-HB and 3-HV production. Despite the lack of metabolite production, cell growth was not significantly inhibited compared to P3HA31. The complimentary acetate assimilation pathway was inactivated in P3HA31Δ*acs*, which resulted in comparable 3-

HB titer compared to P3HA31, and negligible 3-HV production. Cell growth was not significantly inhibited in P3HA31Δ*acs* compared to P3HA31.

Table 6: Growth data and metabolite profile of P3HA31 and mutants of genes related to the acetate assimilation.

Strain	**Cell density (OD_{600})[a]**	**Acetate consumed (g/L)[b]**	**Metabolites produced (g/L)[c]**		
			3-HB	**3-HV**	**Propionate**
P3HA31 (control)	9.39 ± 0.63	18.3 ± 1.6	0.562 ± 0.044 (3.6%)	0.571 ± 0.053 (4.8%)	2.92 ± 0.67 (25.9%)
P3HA31Δ*pta*	9.2 ± 1.4	8.7 ± 2.4	0.073 ± 0.024 (0.9%)	N.D.[d]	0.092 ± 0.019 (1.7%)
P3HA31Δ*acs*	8.1 ± 0.5	6.9 ± 2.6	0.65 ± 0.07 (11.0%)	N.D.[d]	0.80 ± 0.11 (18.8%)

[a] Measured cell density after 48h cultivation using spectrophotometer (OD_{600}) initial cell densities were kept at ~5.0

[b] Consumed acetate after 48h cultivation (20 g/L initial concentration)

[c] Metabolites produced after 48h cultivation, yield is presented in parentheses as a percentage of theoretical maximum yield based on acetate consumed (%)

[d] No 3-HV was detected as the 3-HV peak could not be accurately separated from the acetate peak

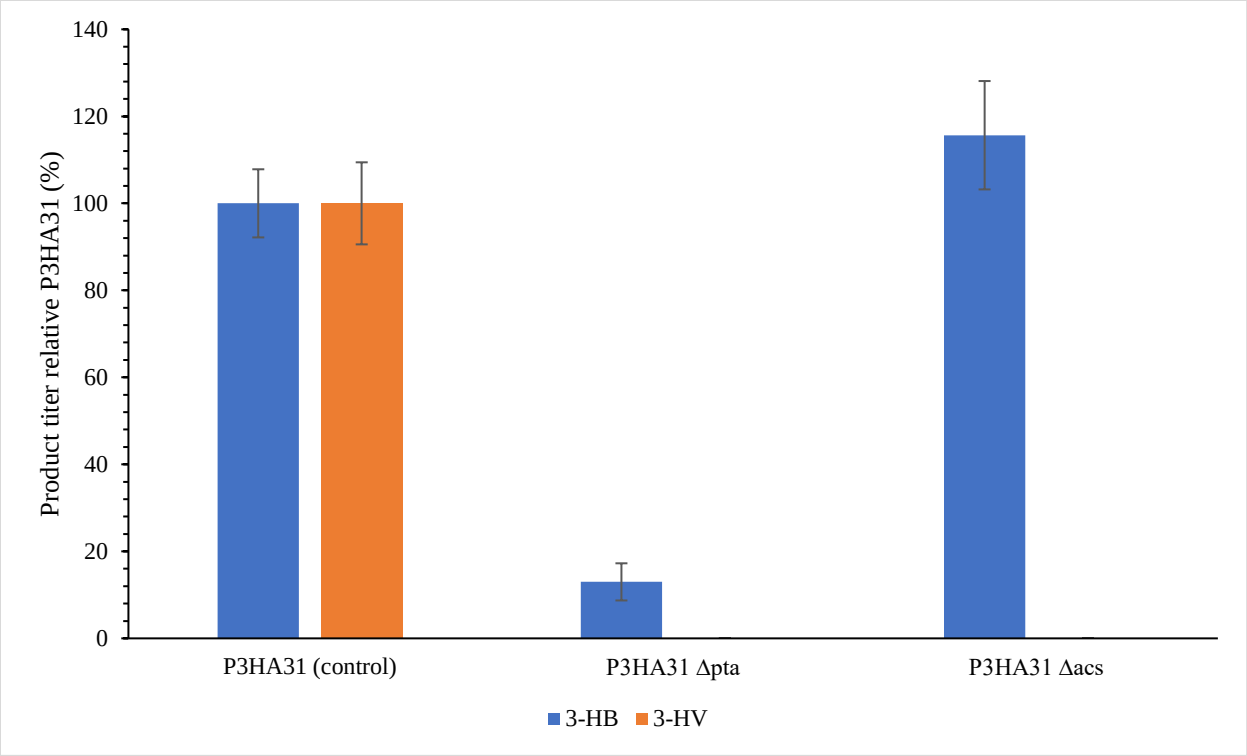

Figure 5: A graph comparing the production of 3-HB and 3-HV relative to P3HA31 for the mutants of genes associated with acetate assimilation.

3.4 - Genetic manipulation of the glyoxylate shunt pathway

The glyoxylate shunt pathway can be induced under acetate metabolism, leading to high carbon flux through this pathway (Oh et al., 2002). The growth data and metabolite profile for the genetic manipulation of the glyoxylate shunt can be found in **Table 7** with the relative 3-hydroxyacid productions shown in **Figure 6**. The pathway is derived from the *aceBAK* operon which codes for the isocitrate lyase, AceA, (encoded by *aceA*), the malate synthase, AceB, (encoded by *aceB*), and the isocitrate dehydrogenase kinase/phosphatase, AceK, (encoded by *aceK*). AceA decomposes isocitrate to form glyoxylate and succinate. AceB fuses acetyl-CoA and glyoxylate to form malate, serving as a route for acetyl-CoA to enter the TCA cycle. AceK acts to phosphorylate the isocitrate dehydrogenase, Icd (encoded by *icd*), inhibiting its activity. In P3HA31Δ*aceB* the cell growth was inhibited, however the 3-HB titer for this mutant was comparable to the 3-HB titer of P3HA31. *E.*

coli possesses a second malate synthase, GlcB, (encoded by *glcB*), which is involved in glycolate and glyoxylate metabolism pathways. P3HA31Δ*glcB* also produced comparable levels of 3-HB to that of the P3HA31, yet did not inhibit cell growth as significantly as P3HA31Δ*aceB.* The double mutant P3HA31Δ*aceB*Δ*glcB* removed the activity of both malate synthases resulting in a 2.6-fold increase in 3-HB titer over the P3HA31, despite significantly inhibited cell growth. The activity of the DNA-binding transcriptional repressor for the *aceBAK* operon, IclR, (encoded by *iclR*) was removed in P3HA31Δ*iclR* and lead to slight reductions in both 3-HV and 3-HB titers, compared to P3HA31. P3HA31Δ*iclR* also had slightly impaired growth compared the P3HA31.

Table 7: Growth data and metabolite profile of P3HA31 and mutants of genes related to the glyoxylate shunt.

Strain	**Cell density (OD_{600})[a]**	**Acetate consumed (g/L)[b]**	**Metabolites produced (g/L)[c]**		
			3-HB	**3-HV**	**Propionate**
P3HA31 (control)	9.39 ± 0.63	18.3 ± 1.6	0.562 ± 0.044 (3.6%)	0.571 ± 0.053 (4.8%)	2.92 ± 0.67 (25.9%)
P3HA31Δ*aceB*	7.38 ± 0.28	7.4 ± 1.5	0.45 ± 0.11 (7.0%)	N.D.[d]	0.40 ± 0.08 (8.8%)
P3HA31Δ*glcB*	8.7 ± 1.1	10.0 ± 3.0	0.74 ± 0.21 (8.4%)	N.D.[d]	1.0 ± 0.8 (16.0%)
P3HA31Δ*aceB*Δ*glcB*	6.82 ± 0.33	10.0 ± 3.5	1.40 ± 0.19 (15.8%)	N.D.[d]	0.49 ± 0.33 (7.9%)
P3HA31Δ*iclR*	8.38 ± 0.09	7.96 ± 0.16	0.45 ± 0.05 (6.4%)	0.362 ± 0.002 (6.8%)	0.66 ± 0.09 (13.4%)

[a] Measured cell density after 48h cultivation using spectrophotometer (OD_{600}) initial cell densities were kept at ~5.0

[b] Consumed acetate after 48h cultivation (20 g/L initial concentration)

[c] Metabolites produced after 48h cultivation, yield is presented in parentheses as a percentage of theoretical maximum yield based on acetate consumed (%)

[d] No 3-HV was detected as the 3-HV peak could not be accurately separated from the acetate peak

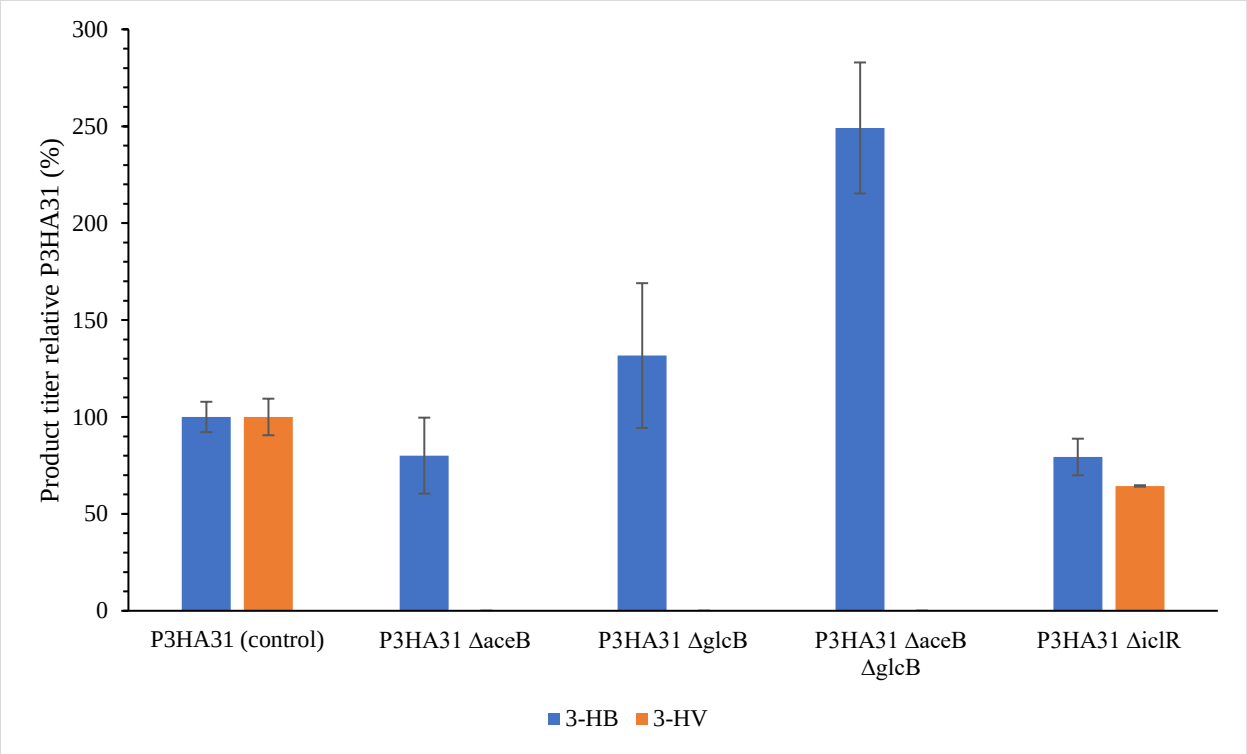

Figure 6: A graph comparing the production of 3-HB and 3-HV relative to P3HA31 for the mutants of genes associated with the glyoxylate shunt.

3.5 - Genetic manipulation of the pathways related to the PEP-pyruvate node

The PEP-pyruvate node serves as a complex interchange of glycolytic and gluconeogenic pathways, as well as carbon exchange between these pathways and the TCA cycle. The results of the gene knockouts related to the PEP-pyruvate node are given in **Table 8** with the relative 3-hydroxy acid productions shown in **Figure 7**. Pyruvate may be generated directly from malate by either of two malate dehydrogenases, SfcA, and MaeB (encoded by *sfcA* and *maeB* respectively). The malate dehydrogenases differ in their reducing equivalent production; SfcA is NADH-producing while MaeB is NADPH-producing. P3HA31Δ*sfcA* produced negligible amounts of either 3-hydroxy acids, whereas P3HA31Δ*maeB* produced less 3-HB compared to P3HA31 and negligible amounts of 3-HV. Both P3HA31Δ*sfcA* and P3HA31Δ*maeB* had slightly inhibited cell growth compared to P3HA31. PEP can be generated from oxaloacetate (OAA) by the PEP

carboxykinase, PckA (encoded by *pckA*). The removal of PckA activity in P3HA31Δ*pckA* did not significantly affect cell growth or 3-HB titer while exhibiting a slight decrease in 3-HV titer compared to P3HA31. PEP can be returned to the TCA cycle via the activity of Ppc (encoded by *ppc)* producing OAA. Removing the activity of Ppc in P3HA31Δ*ppc*, resulted in a significant decrease in 3-HB titer compared to P3HA31 and negligible 3-HV production. P3HA31Δ*ppc* did not significantly affect cell growth compared P3HA31. The inter-conversion of pyruvate and PEP are maintained by the PEP synthetase, PpsA, (encoded by *ppsA*) and the pyruvate kinase, PykF, (encoded by *pykF*). PykF catalyzes the conversion of PEP to pyruvate (producing ATP), whereas the conversion of pyruvate to PEP (requiring ATP) is catalyzed by PpsA. P3HA31Δ*pykF* did not have a significant effect on either 3-HB or 3-HV titers, and slightly inhibited cell growth compared to P3HA31. P3HA31Δ*ppsA* produced approximately a 1.5-fold higher titer of 3-HB compared to P3HA31, while also producing negligible amounts of odd-chained metabolites (3-HV and propionate). Removal of PpsA activity did not significantly affect cell growth. P3HA31Δ*aceF* removed the activity of AceF (encoded by *aceF*), a critical subunit of the aerobic pyruvate dehydrogenase complex (AceEF). This mutant exhibited significant growth deficiencies in LB media, however when cultivated in acetate media the growth was restored and OD_{600} exceeded that of P3HA31. P3HA31Δ*aceF* also yielded a 1.9-fold increase in 3-HB titer and a significant decrease in 3-HV titer. Catalyzing a similar reaction, the activity of pyruvate formate lyase, PflB, (encoded by p*flB*) was removed in P3HA31Δ*pflB*. This resulted in insignificant changes in 3-HB and 3-HV titers while slightly inhibiting cell growth.

Table 8: Growth data and metabolite profile of P3HA31 and mutants of genes related to the PEP-pyruvate node.

Strain	**Cell density (OD_{600})[a]**	**Acetate consumed (g/L)[b]**	**Metabolites produced (g/L)[c]**		
			3-HB	**3-HV**	**Propionate**
P3HA31 (control)	9.39 ± 0.63	18.3 ± 1.6	0.562 ± 0.044 (3.6%)	0.571 ± 0.053 (4.8%)	2.92 ± 0.67 (25.9%)
P3HA31Δ*sfcA*	7.37 ± 0.44	10.4 ± 1.4	0.057 ± 0.014 (0.6%)	N.D.[d]	1.21 ± 0.09 (18.9%)
P3HA31Δ*maeB*	8.40 ± 0.31	7.00 ± 0.47	0.357 ± 0.014 (5.8%)	N.D.[d]	0.67 ± 0.06 (15.4%)
P3HA31Δ*pckA*	8.51 ± 0.32	9.7 ± 1.8	0.510 ± 0.018 (6.0%)	0.403 ± 0.024 (6.3%)	0.89 ± 0.31 (15.0%)
P3HA31Δ*ppc*	8.85 ± 0.13	11.6 ± 3.5	0.164 ± 0.007 (1.6%)	N.D.[d]	1.6 ± 0.6 (22.4%)
P3HA31Δ*pykF*	8.27 ± 0.50	8.4 ± 2.9	0.56 ± 0.08 (7.6%)	0.53 ± 0.11 (9.5%)	0.76 ± 0.41 (14.7%)
P3HA31Δ*ppsA*	8.82 ± 0.23	8.1 ± 1.1	0.84 ± 0.05 (12.1%)	N.D.[d]	0 (0%)
P3HA31Δ*aceF*	11.96 ± 0.06	~20	0.99 ± 0.07 (5.7%)	0.234 ± 0.034 (1.8%)	1.06 ± 0.02 (8.6%)
P3HA31Δ*pflB*	8.29 ± 0.62	11.6 ± 0.9	0.44 ± 0.11 (4.3%)	0.42 ± 0.1 (5.5%)	1.1 ± 0.6 (14.6%)

[a] Measured cell density after 48h cultivation using spectrophotometer (OD_{600}) initial cell densities were kept at ~5.0

[b] Consumed acetate after 48h cultivation (20 g/L initial concentration)

[c] Metabolites produced after 48h cultivation, yield is presented in parentheses as a percentage of theoretical maximum yield based on acetate consumed (%)

[d] No 3-HV was detected as the 3-HV peak could not be accurately separated from the acetate peak

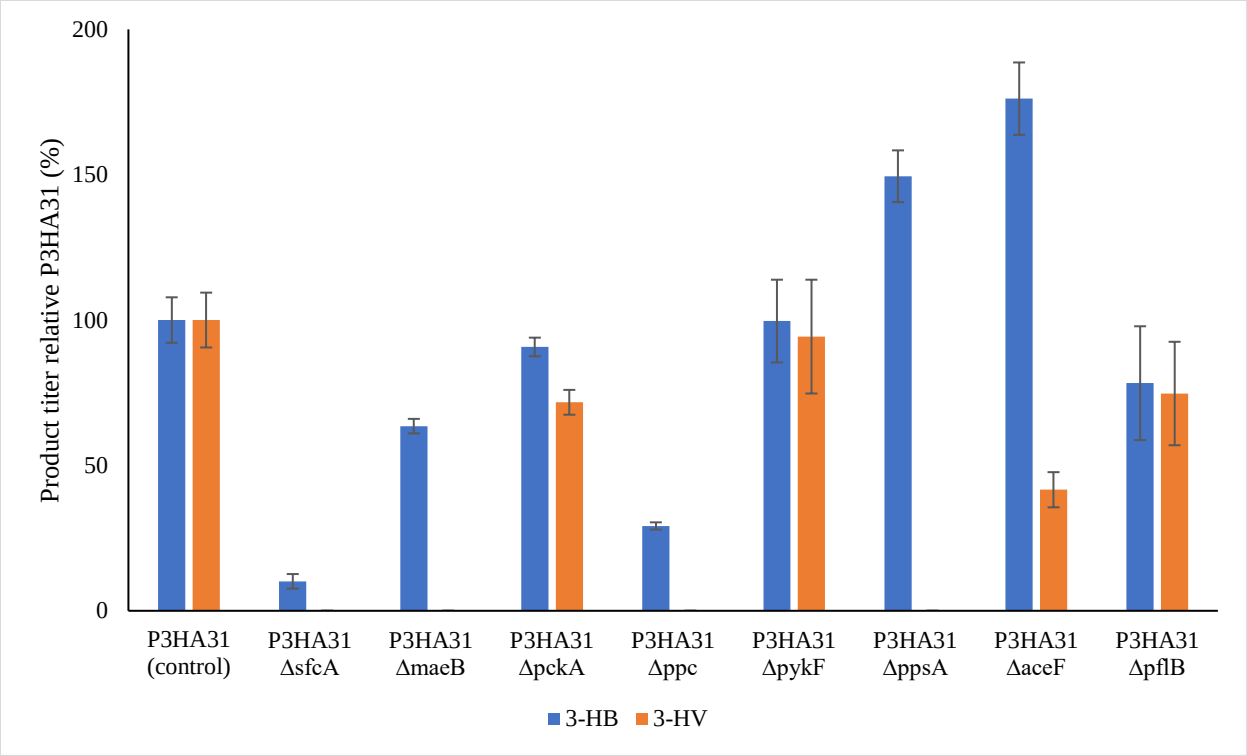

Figure 7: A graph comparing the production of 3-HB and 3-HV relative to P3HA31 for the mutants of genes associated with the PEP-pyruvate node.

3.6 - Genetic manipulation of global regulator systems

Four global regulator enzymes (ArcA, Fnr, CreB, and CreC) were examined via gene knockouts and the results are shown in **Table 9**. Also, the relative 3-hydroxy acid productions of these knockouts are shown in **Figure 8.** These regulator systems affect multiple different enzymes and pathways depending on environmental conditions such as oxygen and carbon source availability. Inactivation of *arcA*, which encodes for the DNA-binding transcriptional regulator, ArcA, resulted in a 3.2-fold increase in 3-HB titer and significant reduction in 3-HV titer compared to P3HA31. Cell growth was significantly inhibited in P3HA31Δ*arcA* compared to P3HA31. Another DNA-binding transcriptional regulator, Fnr (encoded by *fnr*), was inactivated in P3HA31Δ*fnr*, which had a 2.1-fold increase in 3-HB titer and a significantly reduced 3-HV titer compared to P3HA31. Cell growth was not significantly affected in P3HA31Δ*fnr*. The CreBC regulator system is a

carbon source sensitive, two-component regulator system, where the sensory kinase, CreC, (encoded by *creC*) phosphorylates the DNA-binding transcriptional regulator, CreB, (encoded by *creB*) activating it. The CreBC regulator system is presumed to be inactive in both P3HA31Δ*creB* and P3HA31Δ*creC* (Cariss et al., 2008). P3HA31Δ*creB* had similar 3-HB and 3-HV titers to what was observed in P3HA31 while P3HA31Δ*creC* increased 3-HB titer by 1.3-fold, with no significant 3-HV production. Both P3HA31Δ*creB* and P3HA31Δ*creC* had significantly lower cell growth than the P3HA31.

Table 9: Growth data and metabolite profile of P3HA31 and mutants of genes coding for global regulators.

Strain	**Cell density (OD_{600})[a]**	**Acetate consumed (g/L)[b]**	**Metabolites produced (g/L)[c]**		
			3-HB	**3-HV**	**Propionate**
P3HA31 (control)	9.39 ± 0.63	18.3 ± 1.6	0.562 ± 0.044 (3.6%)	0.571 ± 0.053 (4.8%)	2.92 ± 0.67 (25.9%)
P3HA31Δ*arcA*	7.38 ± 0.11	14.1 ± 1.1	1.75 ± 0.05 (14.1%)	0.32 ± 0.04 (3.5%)	1.58 ± 0.04 (18.2%)
P3HA31Δ*fnr*	8.1 ± 1.1	17 ± 3	1.14 ± 0.11 (7.6%)	0.31 ± 0.03 (2.7%)	1.13 ± 0.50 (10.8%)
P3HA31Δ*creB*	7.71 ± 0.10	6.6 ± 1.3	0.513 ± 0.006 (8.8%)	0.49 ± 0.15 (11.2%)	0.583 ± 0.039 (14.3%)
P3HA31Δ*creC*	7.71 ± 0.34	6.6 ± 1.8	0.757 ± 0.050 (13.0%)	N.D.[d]	0.55 ± 0.17 (13.4%)

[a] Measured cell density after 48h cultivation using spectrophotometer (OD_{600}) initial cell densities were kept at ~5.0

[b] Consumed acetate after 48h cultivation (20 g/L initial concentration)

[c] Metabolites produced after 48h cultivation, yield is presented in parentheses as a percentage of theoretical maximum yield based on acetate consumed (%)

[d] No 3-HV was detected as the 3-HV peak could not be accurately separated from the acetate peak

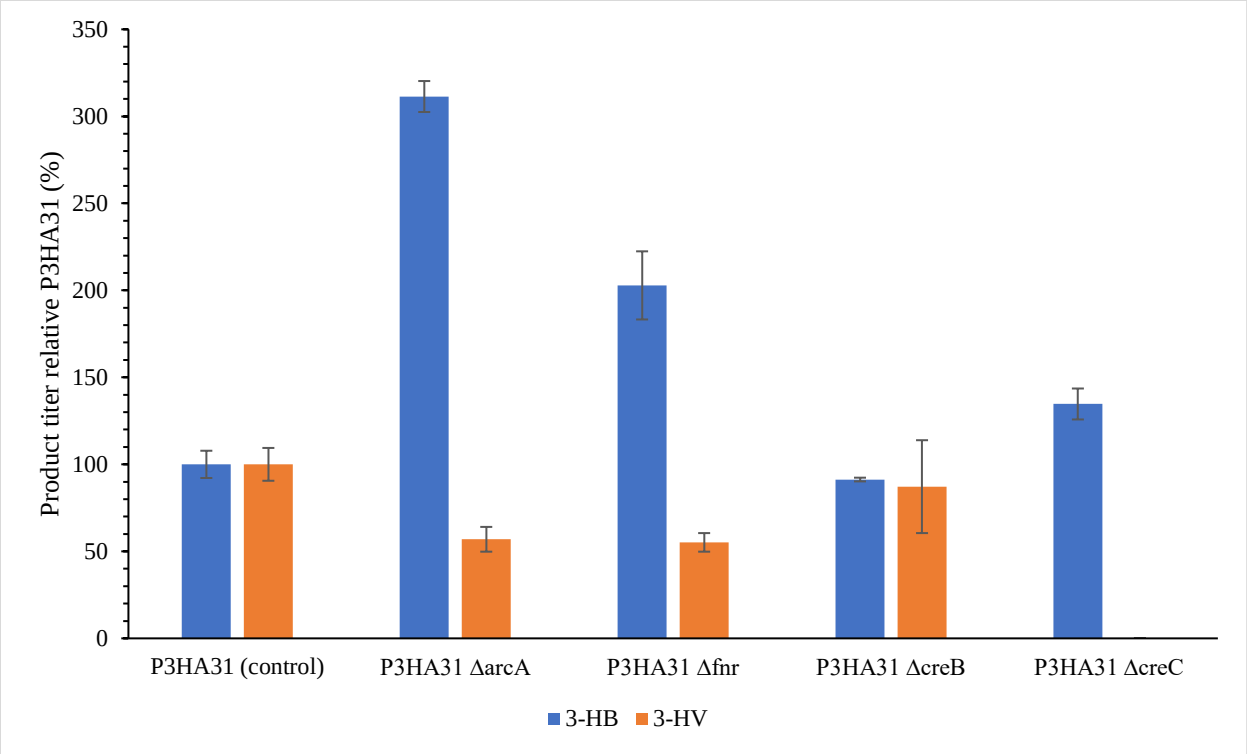

Figure 8: A graph comparing the production of 3-HB and 3-HV relative to P3HA31 for the mutants of genes coding for global regulators.

Chapter 4 – Discussion

Cultivation conditions, i.e. temperature and carbon source concentration, were initially studied in order to develop a standard procedure for subsequent gene knockout cultivations, while improving 3-hydroxy acid production and acetate consumption in P3HA31. The effect of temperature was observed when P3HA31 was grown at both 30˚C and 37˚C. As shown in **Table 4**, the 3-HV titer was considerably higher at 30˚C compared to 37˚C, while 3-HB titer was also slightly increased at 30˚C. Previous experiments concerning propionyl-CoA derived products suggest enhanced carbon flux through the Sbm pathway at 30˚C (Miscevic, 2018). This suggestion is also supported by the significantly increased propionate titer of P3HA31 at 30˚C compared to 37˚C. Initial acetate concentration in the cultivation media was also investigated with the results shown in **Table 5**. At

high concentrations (at 30 g/L of acetate), cell growth and acetate consumption were dramatically reduced. The cultivation media is fixed to an initial pH of 7, meaning both protonated acetic acid and ionized acetate are present in solution. The protonated acetic acid is lipophilic and can pass through the cell membrane then dissociate in the alkaline cytoplasm (pH of ~7.4) decreasing the intracellular pH (Luli & Strohl, 1990). To maintain homeostasis within the cells, energy is required via the proton motive force to maintain sufficient intracellular pH (Luli & Strohl, 1990). Additionally, anionic metabolites such as glutamate must be excreted to exchange for the acetate ions in the cytoplasm, in order to maintain electroneutrality across the cell membrane (Roe et al., 1998). These mechanisms lead to cell growth inhibition in the presence of acetate media, with the inhibition effects being exacerbated at higher acetate concentrations. Therefore, the standard cultivation conditions were set at 30˚C with 20 g/L acetate media for investigating the effects of genetic manipulations.

Acetate assimilation in *E. coli* occurs by two distinct pathways, the AckA-Pta pathway, or via the Acs enzyme. The significance of each pathway for acetate assimilation is dependent on extracellular acetate concentration. Acs has a high affinity for acetate (K_M = 200 μM) and is functional under scavenging conditions with low acetate concentrations. The enzymes Pta and AckA have comparatively low substrate affinity (K_M = 7-10 mM) and are predominantly effective for acetate metabolism at high acetate concentrations (Wolfe, 2005). During growth on acetate as the sole carbon source, both pathways should be active with AckA-Pta being responsible for initial acetate consumption, while Acs becomes more active towards the end of the cultivations when acetate concentrations are low. It should be noted the Acs pathway also converts ATP to AMP, whereas the AckA-Pta pathway converts ATP to ADP during their production of acetyl-CoA. Removing the AckA-Pta pathway activity in P3HA31Δ*pta* did not significantly affect cell growth

but did decrease acetate consumption as well as caused negligible metabolite production. This could suggest that the Acs pathway can sufficiently assimilate acetate to maintain cell growth but requires excessive energy (in the form of ATP to AMP conversion) that metabolite production is significantly hindered. This hypothesis of energy dependence is also supported by the slightly increased 3-HB production observed in P3HA31Δ*acs*. By removing the Acs pathway function, acetate assimilation favors the more energy efficient AckA-Pta pathway, which could lead to the increased 3-HB production.

The glyoxylate shunt pathway is highly active under acetate metabolism (Oh et al., 2002) acting as a route to incorporate acetyl-CoA into the TCA cycle, as well as bypassing the carbon dioxide producing steps of the TCA cycle. By removing each malate synthase activity in P3HA31Δ*aceB* and P3HA31Δ*glcB* individually, no significant effect in 3-HB titer was observed. Although the malate synthases are genetically and structurally independent, both are active under acetate metabolism (Oh et al., 2002; Pellicer et al., 1999). As a result, when one malate synthase is inactivated the other can maintain carbon flux through glyoxylate bypass pathway (Pellicer et al., 1999). However, in P3HA31Δ*aceB*Δ*glcB* activity of both malate synthases were removed and the mutant produced a significantly increased 3-HB titer. AceB and GlcB each act on acetyl-CoA and are competitive with the 3-hydroxy acid pathways. Therefore, when this competitive pathway is no longer active in P3HA31Δ*aceB*Δ*glcB*, more carbon flux can be directed towards 3-HB production. Conversely, the removal of IclR activity in P3HA31Δ*iclR* would allow increased expression of the *aceBAK* operon resulting in increased carbon flux through the glyoxylate shunt. The increased expression of AceB could enhance acetyl-CoA consumption through the glyoxylate shunt. This could result in the decrease in 3-HB and 3-HV production observed in P3HA31Δ*iclR*, due to the decreased acetyl-CoA pool.

The major route for pyruvate production is via the two malate dehydrogenases, the NADH-producing SfcA and the NADPH-producing MaeB. P3HA31Δ*maeB* observed decreased 3-HB and 3-HV titres, however no significant 3-HB or 3-HV production was observed in P3HA31Δ*sfcA*. During growth on acetate NADPH can be generated in excess via, the Icd catalyzed conversion of isocitrate to 2-ketoglutarate, whereas NADH is limiting by comparison (Clark & Cronan, 1996). This could suggest the apparent requirement of SfcA in order to produce NADH during growth on acetate, whereas MaeB is not required for NADPH production. Since 3-hydroxy acid synthesis pathways require both NADH and NADPH, the inhibited NADH production in P3HA31Δ*sfcA* could drastically decrease 3-hydroxy acid productions. PckA serves as a separate route to the PEP-pyruvate node from TCA intermediates by catalyzing the production of PEP from OAA. The removal of PckA activity in P3HA31Δ*pckA* did not yield a significant change in 3-HB titer and only a slight decrease in 3-HV titer. In the absence of PckA, the PEP pool can be maintained via the SfcA/MaeB and PpsA pathway under growth on acetate (Oh et al., 2002), suggesting PckA is not required for acetate metabolism. Similarly, PckA can provide sufficient PEP production when the activity of PpsA is removed. However, it has been shown that deletion of the *ppsA* gene can affect the expression of specific global regulators (Kao et al., 2005), which may have caused the apparent inhibition of the Sbm pathway. This could result in the lack of odd-chain metabolite (3-HV and propionate) production observed for P3HA31Δ*ppsA*. An inactive Sbm pathway would not allow any propionyl-CoA production thereby preventing propionate or 3-HV production. The absence of propionyl-CoA could also result in increased 3-HB production by removing the 3-HV pathway, which is in competition for acetyl-CoA. The removal of Ppc activity resulted in significantly decreased production of both 3-hydroxy acids, however propionate production was only slightly lower than in P3HA31. Enzyme activity assays of *E. coli* mutants lacking *ppc* gene

have shown an upregulation of GltA, Icd, AceA, and Mdh enzymes resulting in increased flux through the TCA cycle and glyoxylate shunt (Peng & Shimizu 2004). These pathways direct carbon flux towards the Sbm pathway while also competing for acetyl-CoA. This could lead to a decrease of intracellular acetyl-CoA concentration in *ppc* deletion mutants (Peng & Shimizu 2004), which could result in the decreased production of 3-hydroxy acids. P3HA31Δ*pykF* did not exhibit any significant change in 3-hydroxy acid titers compared to P3HA31. The results suggest PykF is not critical for acetate metabolism, which is supported by the down-regulation of *pykF* during growth on acetate (Oh et al., 2002). Removal of AceEF activity adversely affects the aerobic growth of *E. coli*, however growth can be restored with acetate supplementation (Clark & Cronan, 1996). Therefore, it's suggested that AceEF is required for production of acetyl-CoA from structurally unrelated carbon sources. In the case of acetate metabolism, acetyl-CoA would be directly produced from acetate and the AceEF-mediated conversion from pyruvate forms a futile loop. P3HA31Δ*aceF* breaks this futile loop and prevents the energy and carbon loss associated. This in turn allows pyruvate accumulation (Tomar et al., 2003) that could be repurposed towards biomass production resulting in the increased cell density in P3HA31Δ*aceF* when compared to P3HA31. The carbon and energy conservation associated with breaking the futile loop could also contribute to increased production of 3-HB. Similarly, PflB causes the futile loop converting pyruvate to acetyl-CoA under anaerobic growth. However, growth conditions in the shaker are not strictly anaerobic resulting in low PflB activity. Due to the low activity of PflB under the shaker conditions, P3HA31Δ*pflB* did not significantly affect 3-hydroxy acid titers.

Global regulators affect gene expression for various pathways making them important targets for genetic manipulations. These regulators bind to specific markers of affected genes to either inhibit or activate transcription of affected genes to regulate their expression. Removal of

either ArcA or Fnr activity, produced significantly higher titers of 3-HB and significantly lower titers of 3-HV compared to P3HA31. ArcA is active during the transition of aerobic to micro-aerobic growth, whereas, Fnr is predominantly active during the transition to anaerobic growth (Shalel Levanon et al., 2005). The results suggest that by removing the activity of these regulators, cells would not transition from aerobic growth to microaerobic or anaerobic growth while available oxygen in the shaker environment decreased. The continued aerobic growth could cause accumulation of the acetyl-CoA pool leading to the increased 3-HB production. It has also been suggested that P3HA31Δ*arcA* mutants possess higher NADH/NAD^+ ratios than in wild-type cells (Shalel-Levanon et al., 2005). The increased NADH pool could enhance flux through the NADH-dependent 3-hydroxy acid pathways leading to further increases in the 3-HB titer. The CreBC regulator system has been shown to be activated under aerobic growth on acetate (Cariss et al., 2008). The CreBC regulator system activates the expression of the *ackA* gene (Avison et al., 2001; Godoy et al., 2016). Since AckA is critical in acetate assimilation its decreased expression under P3HA31Δ*creB* and P3HA31Δ*creC* mutants would cause the reduced carbon consumption rates observed in these mutants. The CreBC regulator system may be involved in the expression of other genes related to acetate metabolism allowing acetyl-CoA accumulation despite low acetate consumption leading to the unaffected and slightly increased 3-HB titers observed in P3HA31Δ*creB* and P3HA31Δ*creC* respectively.

Chapter 5 – Conclusions

In conclusion, this study has demonstrated that both 3-HB and 3-HV can be effectively produced using acetate as a feedstock. Manipulations of culture conditions resulted in increased production of 3-HB and 3-HV at 30˚C compared 37˚C. Additionally, inhibition of cell growth and product formation was observed when using 30 g/L acetate in the initial media, however this inhibition

was not observed when using 20 g/L acetate in the initial media. Genetic manipulations of acetate metabolism pathways suggest theories to affect 3-hydroxy acid productions: i) 3-HB production appears to be dependant on acetyl-CoA availability as the elimination of non-essential acetyl-CoA-consuming pathways increased 3-HB titre. Additionally, increases in acetyl-CoA consumption by competitive pathways resulted in decreased 3-HB titre ii) 3-HV production appears to require a balance of both acetyl-CoA and propionyl-CoA precursors. It is thought that this balance is best achieved in the control strain, P3HA31, as all genetic manipulations resulted in a decreased 3-HV titer iii) Accumulation and efficient use of reducing equivalents (NADH/NADPH) and energy (ATP) are also important for 3-hydroxy acid formation. Further research into production of 3-hydroxy acids using acetate feedstock could be directed towards gene overexpressions to increase acetate assimilation, supplementations to increase intracellular reducing equivalents and/or energy, or developing a more acetate-tolerant strain to limit the inhibitory effects at high concentrations of acetate.

Chapter 6 – Future applications of 3-hydroxy acid production using acetate

As mentioned previously, 3-HB and 3-HV can be used as monomers for production of the biopolymer, PHBV. Previous studies have demonstrated the production of PHBV using CPC-Sbm containing a two-plasmid system for heterologous expression of the PHBV production pathway (this strain is referred to as CPC-PHBV) (Srirangan et al., 2016). The authors in this study demonstrate a similar metabolic pathway for PHBV production to that which has been discussed for 3-hydroxy acid formation (**Figure 9**). This pathway relies on the polyhydroxyalkanoate polymerase, PhaC (encoded by *phaC* from *C. necator*) to fuse 3-HB-CoA and 3-HV-CoA to produce PHBV in place of TesB (for 3-hydroxy acid production). Additionally, PhaC is selective for only the (*R*) enantiomer eliminating the need of Hbd for (*S*) enantiomer production. The authors

reported production of 6.8 g/L of PHBV with 7.2mol% 3-HV monomer, using a batch bioreactor under semiaerobic aeration conditions with 30 g/L glycerol as the carbon source. Interestingly, the authors also reported production of approximately 6 g/L of acetate during cultivation. We performed a similar cultivation using CPC-PHBV growing on acetate as the sole carbon source. The results for this experiment compared to the previously reported values can be found in **Table 10.** We demonstrated that under microaerobic aeration conditions CPC-PHBV can produce 6.4 g/L of PHBV with 11.7mol% 3-HV monomer using 20 g/L acetate as a carbon source. These results could suggest an opportunity of using the waste acetate from the cell-free bioreactor effluent for a secondary cultivation to increase PHBV production. Additionally, results of this thesis project could be used to metabolically engineer CPC-PHBV to increase biopolymer production or affect the composition of the biopolymer.

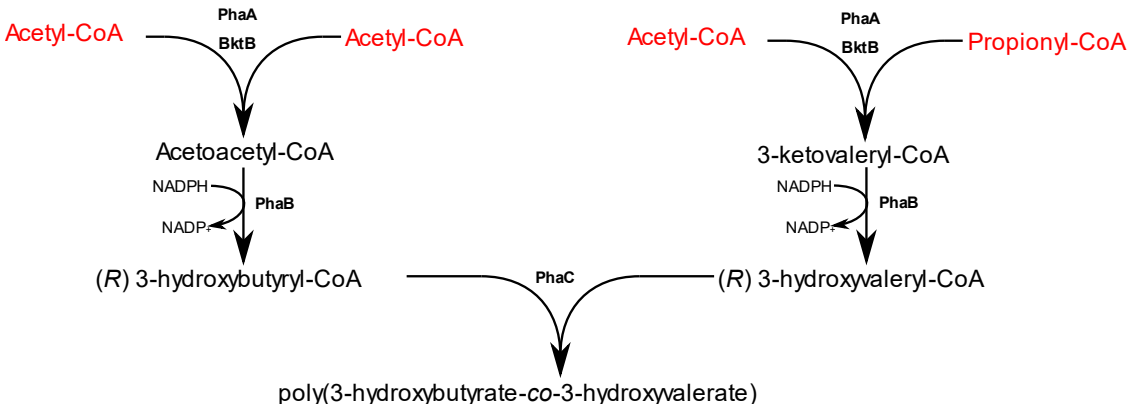

Figure 9: Heterologous PHBV pathway from acetyl-CoA and propionyl-CoA precursors. Enzyme abbreviations: PhaA, acetoacetyl-CoA thiolase (from *C. necator*); BktB, ß-ketothiolase (from *C. necator*); PhaB, acetoacetyl-CoA reductase (from *C. necator*); PhaC, polyhydroxyalkanoate polymerase (from *C. necator*).

Table 10: Comparison of biopolymer content and composition for PHBV production reported in a previous study using glycerol as a carbon source versus experimental PHBV production using acetate as a carbon source.

Study	Feedstock	Aeration condition	OD_{600}[a]	Dry cell weight (g/L)	Biopolymer content (g/L)	3-HV content (mol%)
(Srirangan et al., 2016)	30g/L glycerol	Semiaerobic[b]	Not specified	11	6.8	7.2
This study	20 g/L acetate	Microaerobic[c]	27.3	8.5 ± 0.1	6.40 ± 0.34	11.7 ± 0.1

[a] Sample for analysis was taken when all acetate was consumed.

[b] Semiaerobic condition achieved by sparging air into the bulk culture at 0.1 vvm

[c] Microaerobic condition achieved by purging air into the bioreactor headspace at 0.1 vvm

References

Akawi, L., Srirangan, K., Liu, X., Moo-Young, M., & Chou, C. P. (2015). Engineering Escherichia coli for high-level production of propionate. *Journal of industrial microbiology & biotechnology, 42*(7), 1057-1072.

Amann, E., Ochs, B., & Abel, K.-J. (1988). Tightly regulated tac promoter vectors useful for the expression of unfused and fused proteins in Escherichia coli. *Gene, 69*(2), 301-315.

Avison, M. B., Horton, R. E., Walsh, T. R., & Bennett, P. M. (2001). Escherichia coli CreBC is a global regulator of gene expression that responds to growth in minimal media. *Journal of Biological Chemistry, 276*(29), 26955-26961.

Baba, T., Ara, T., Hasegawa, M., Takai, Y., Okumura, Y., Baba, M., . . . Mori, H. (2006). Construction of Escherichia coli K-12 in-frame, single-gene knockout mutants: the Keio collection. *Molecular systems biology, 2*(1).

Biernacki, M., Riechen, J., Hahnel, U., Roick, T., Baronian, K., Bode, R., & Kunze, G. (2017). Production of (R)-3-hydroxybutyric acid by *Arxula adeninivorans*. *AMB Express, 7*(4)

Cariss, S. J. L., Tayler, A. E., & Avison, M. B. (2008). Defining the growth conditions and promoter-proximal DNA sequences required for activation of gene expression by CreBC in Escherichia coli. *Journal of bacteriology, 190*(11), 3930-3939.

Casadaban, M. J. (1976). Transposition and fusion of the lac genes to selected promoters in Escherichia coli using bacteriophage lambda and Mu. *Journal of molecular biology, 104*(3), 541-555.

Castaño-Cerezo, S., Pastor, J. M., Renilla, S., Bernal, V., Iborra, J. L., & Cánovas, M. J. M. c. f. (2009). An insight into the role of phosphotransacetylase (pta) and the acetate/acetyl-CoA node in Escherichia coli. *8*(1), 54.

Chaaban, J. H., Dam-Johansen, K., Skovby, T., Kiil, S. (2014). Separation of Enantiomers by Preferential Crystallization: Mathematical Modeling of a Coupled Crystallizer Configuration. *Organic Process Research & Development, 18*,601-12.

Cherepanov, P. P., & Wackernagel, W. (1995). Gene disruption in Escherichia coli: Tc R and Km R cassettes with the option of Flp-catalyzed excision of the antibiotic-resistance determinant. *Gene, 158*(1), 9-14.

Chong, H., Yeow, J., Wang, I., Song, H., & Jiang, R. (2013). Improving acetate tolerance of Escherichia coli by rewiring its global regulator cAMP receptor protein (CRP). *PloS one, 8*(10), e77422.

Clark, D. P., & Cronan, J. E. (1996). Two-carbon compounds and fatty acids as carbon sources. *Escherichia coli and Salmonella: cellular and molecular biology, 2nd ed. ASM Press, Washington, DC*, 343-357.

Cybulski, A., Sharma, M., Sheldon, R., & Moulijn, J. (2001). *Fine Chemicals Manufacture: Technology and Engineering*: Gulf Professional Publishing.

Datsenko, K. A., & Wanner, B. L. (2000). One-step inactivation of chromosomal genes in Escherichia coli K-12 using PCR products. *Proceedings of the National Academy of Sciences, 97*(12), 6640-6645.

De Mey, M., De Maeseneire, S., Soetaert, W., & Vandamme, E. (2007). Minimizing acetate formation in E. coli fermentations. *Journal of industrial microbiology & biotechnology, 34*(11), 689-700. doi: 10.1007/s10295-007-0244-2

Doi, Y., Tamaki, A., Kunioka, M., & Soga, K. (1988). Production of copolyesters of 3-hydroxybutyrate and 3-hydroxyvalerate by Alcaligenes eutrophus from butyric and pentanoic acids. *Applied microbiology and biotechnology, 28*(4-5), 330-334.

Gao, H., Wu, Q., & Chen, G. (2002). Enhanced production of D-(-)-3-hydroxybutyric acid by recombinant *Escherichia coli*. *FEMS Microbiology Letters, 213*(1), 59-65

Gavrilescu, M., & Chisti, Y. (2005). Biotechnology—a sustainable alternative for chemical industry. *Biotechnology advances, 23*(7-8), 471-499.

Gibson, D. G., Young, L., Chuang, R.-Y., Venter, J. C., Hutchison III, C. A., & Smith, H. O. (2009). Enzymatic assembly of DNA molecules up to several hundred kilobases. *Nature methods, 6*(5), 343.

Gimenez, R., Nuñez, M. F., Badia, J., Aguilar, J., & Baldoma, L. J. J. o. b. (2003). The gene yjcG, cotranscribed with the gene acs, encodes an acetate permease in Escherichia coli. *185*(21), 6448-6455.

Godoy, M. S., Nikel, P. I., Gomez, J. G. C., & Pettinari, M. J. (2016). The CreC regulator of Escherichia coli, a new target for metabolic manipulations. *Applied and environmental microbiology, 82*(1), 244-254.

Huang, B., Yang, H., Fang, G., Zhang, X., Wu, H., Li, Z., & Ye, Q. (2018). Central pathway engineering for enhanced succinate biosynthesis from acetate in Escherichia coli. *Biotechnology and bioengineering, 115*(4), 943-954.

Ianni, F., Pataj, Z., Gross, H., Sardella, R., Natalini, B., Lindner, W., & Lammerhofer, M. (2014). Direct enantioseparation of underivatized aliphatic 3-hydroxyalkanoic acids with a quinine-based zwitterionic chiral stationary phase. *Journal of Chromatography A, 1363*,101-8

Jobling, M. G., & Holmes, R. K. (1990). Construction of vectors with the p15a replicon, kanamycin resistance, inducible lacZ alpha and pUC18 or pUC19 multiple cloning sites. *Nucleic acids research, 18*(17), 5315.

Kilpatrick, S. (2017). Exploration of acetate as a feedstock for propionate production in engineered Escherichia coli.*University*

Lee, S. Y., & Lee, Y. (2003). Metabolic engineering of Escherichia coli for production of enantiomerically pure (R)-(−)-hydroxycarboxylic acids. *Applied and environmental microbiology, 69*(6), 3421-3426.

Leone, S., Sannino, F., Tutino, M. L., Parrilli, E., & Picone, D. (2015). Acetate: friend or foe? Efficient production of a sweet protein in Escherichia coli BL21 using acetate as a carbon source. *Microbial cell factories, 14*(1), 106.

Li, Q., Jiang, X., Feng, X., Wang, J., Sun, C., Zhang, H., Xian, M., & Liu, H. (2016) Recovery processes of organic acids from fermentation broths in the biomass-based industry. *J. Microbiol Biotechnology*, *26*(1), 1-8

Li, Y., Huang, B., Wu, H., Li, Z., Ye, Q., & Zhang, Y. P. (2016). Production of succinate from acetate by metabolically engineered Escherichia coli. *ACS synthetic biology*, *5*(11), 1299-1307.

Luli, G. W., & Strohl, W. R. (1990). Comparison of growth, acetate production, and acetate inhibition of Escherichia coli strains in batch and fed-batch fermentations. *Applied and environmental microbiology*, *56*(4), 1004-1011.

Miller, J. (1993). A short course in bacterial genetics: a laboratory manual and handbook for Escherichia coli and related bacteria. *Trends in Biochemical Sciences-Library Compendium*, *18*, 193.

Miscevic, D. (2018). Engineering of *Escherichia coli* for biosynthesis of 3-hydroxyvalerate using unrelated carbon sources. *Unpublished*.

Munasinghe, P. C., & Khanal, S. K. (2010). Biomass-derived syngas fermentation into biofuels: opportunities and challenges. *Bioresource technology*, *101*(13), 5013-5022.

Nielsen, J., & Keasling, J. D. (2016). Engineering cellular metabolism. *Cell*, *164*(6), 1185-1197.

Noh, M. H., Lim, H. G., Woo, S. H., Song, J., & Jung, G. Y. (2018). Production of itaconic acid from acetate by engineering acid-tolerant Escherichia coli W. *Biotechnology and bioengineering*, *115*(3), 729-738.

Oh, M.-K., Rohlin, L., Kao, K. C., & Liao, J. C. (2002). Global expression profiling of acetate-grown Escherichia coli. *Journal of Biological Chemistry*, *277*(15), 13175-13183.

Pellicer, M. T., Fernandez, C., Badía, J., Aguilar, J., Lin, E. C., & Baldomà, L. (1999). Cross-induction of glc and ace Operons ofEscherichia coli Attributable to Pathway Intersection CHARACTERIZATION OF THE glc PROMOTER. *Journal of Biological Chemistry*, *274*(3), 1745-1752.

Roe, A. J., McLaggan, D., Davidson, I., O'Byrne, C., & Booth, I. R. (1998). Perturbation of anion balance during inhibition of growth of Escherichia coli by weak acids. *Journal of bacteriology*, *180*(4), 767-772.

Sá-Pessoa, J., Paiva, S., Ribas, D., Silva, I. J., Viegas, S. C., Arraiano, C. M., & Casal, M. J. B. j. (2013). SATP (YaaH), a succinate–acetate transporter protein in Escherichia coli. *454*(3), 585-595.

Schmidt-Dannert, C. (2017). The future of biologically inspired next-generation factories for chemicals. *Microbial biotechnology*, *10*(5), 1164-1166.

Shalel-Levanon, S., San, K.-Y., & Bennett, G. N. (2005). Effect of oxygen, and ArcA and FNR regulators on the expression of genes related to the electron transfer chain and the TCA cycle in Escherichia coli. *Metabolic engineering*, *7*(5-6), 364-374.

Shalel Levanon, S., San, K. Y., & Bennett, G. N. (2005). Effect of oxygen on the Escherichia coli ArcA and FNR regulation systems and metabolic responses. *Biotechnology and bioengineering*, *89*(5), 556-564.

Srirangan, K., Akawi, L., Liu, X., Westbrook, A., Blondeel, E. J., Aucoin, M. G., . . . Chou, C. P. (2013). Manipulating the sleeping beauty mutase operon for the production of 1-propanol in engineered Escherichia coli. *Biotechnology for biofuels, 6*(1), 139.

Srirangan, K., Liu, X., Tran, T. T., Charles, T. C., Moo-Young, M., & Chou, C. P. J. S. r. (2016). Engineering of Escherichia coli for direct and modulated biosynthesis of poly (3-hydroxybutyrate-co-3-hydroxyvalerate) copolymer using unrelated carbon sources. *6*, 36470.

Srirangan, K., Liu, X., Westbrook, A., Akawi, L., Pyne, M. E., Moo-Young, M., & Chou, C. P. (2014). Biochemical, genetic, and metabolic engineering strategies to enhance coproduction of 1-propanol and ethanol in engineered Escherichia coli. *Applied microbiology and biotechnology, 98*(22), 9499-9515.

Tomar, A., Eiteman, M., & Altman, E. (2003). The effect of acetate pathway mutations on the production of pyruvate in Escherichia coli. *Applied microbiology and biotechnology, 62*(1), 76-82.

Tseng, H.-C., Harwell, C. L., Martin, C. H., & Prather, K. L. (2010). Biosynthesis of chiral 3-hydroxyvalerate from single propionate-unrelated carbon sources in metabolically engineered E. coli. *Microbial cell factories, 9*(1), 96.

Wang, Y., Chen, R., Cai, J., Liu, Z., Zheng, Y., Wang, H., . . . He, N. J. P. O. (2013). Biosynthesis and thermal properties of PHBV produced from levulinic acid by Ralstonia eutropha. *8*(4), e60318.

Wolfe, A. J. (2005). The Acetate Switch. *Microbiology and Molecular Biology Reviews, 69*(1), 12-50. doi: 10.1128/mmbr.69.1.12-50.2005

Zhang, Y.-H. P. (2008). Reviving the carbohydrate economy via multi-product lignocellulose biorefineries. *Journal of industrial microbiology & biotechnology, 35*(5), 367-375.

Zhang, Y.-H. P., Sun, J., & Ma, Y. (2017). Biomanufacturing: history and perspective. *Journal of industrial microbiology & biotechnology, 44*(4-5), 773-784.